SCIENTIFIC REPORTS
nature research

OPEN

Antimicrobial activity of Titanium dioxide and Zinc oxide nanoparticles supported in 4A zeolite and evaluation the morphological characteristic

Maryam Azizi-Lalabadi[1,5,6], Ali Ehsani[2,7*], Baharak Divband[3,8] & Mahmood Alizadeh-Sani[4]

In this study, the antimicrobial activity of titanium dioxide (TiO_2), zinc oxide (ZnO), and TiO_2/ZnO nanoparticles supported into 4A zeolite (4A z) was assessed. Based on antimicrobial experiments, minimum inhibitory concentration (MIC_{90}), minimum bactericidal concentration (MBC), fractional inhibitory concentration (FIC) and disc diffusion test were determined after 24 h of contact with the prepared nanocomposites. These results are in agreements with the results of disc diffusion test. During the experiments, the numbers of viable bacterial cells of *Staphylococcus aureus*, *Pseudomonas fluorescens*, *Listeria monocytogenes* and *Escherichia coli* O_{157}:H_7 decreased significantly. The crystallinity and morphology of nanoparticles were investigated by X-ray diffraction patterns (XRD), elemental mapping at the microstructural level by scanning electron microscopy (SEM) with energy dispersive X-ray spectrometry (EDS), and transmission electron microscopy (TEM). As a result, it was demonstrated that TiO_2/ZnO nanoparticles supported in 4A zeolite could lead to an optimum activity as antimicrobial agents.

Zeolites are microporous, alumino silicate minerals with open three-dimensional framework structures, made up of SiO_4 and AlO_4 tetrahedrons linked by sharing oxygen atoms to form regular intra crystalline cavities and channels of atomic dimensions. Zeolites are commonly used as commercial adsorbents and composites, as well as cation exchangers, molecular sieves and antimicrobial agents[1–3].

Attaching nanoparticles on solid surfaces has been used as a traditional procedure to prepare heterogeneous composites with specific properties. Leaching and aggregation of nanoparticles often lead to composite deactivation[4,5]. In order to overcome these problems, some methods have been proposed including strengthening the metal-support interaction[6,7] and using booster and setting out the morphology of nanoparticles[8,9]. Based on these advances, nanoparticles can be loaded on zeolites for antimicrobials, anti-fungal and anti-virus applications[10,11]. These achievements convinced researchers to produce nanoparticles inside zeolite. The new composite (zeolite with nanoparticles) can be tuned through the presence of precise nanopores[3,12,13].

The issue of contamination by certain microorganisms in some materials, especially food, enables a significant hazardous pathway for humans. The most important pathogenic bacteria in food for mankind are *Salmonella spp, Escherichia coli* $O_{157}H_7$, *Staphylococcus aureus*, and *Listeria monocytogenes*[3,14]. Metal oxide nanoparticles (MONP)

[1]Students' Research Committee, Department of Food Sciences and Technology, Faculty of Nutrition and Food Sciences, Tabriz University of Medical Sciences, Tabriz, Iran. [2]Nutrition Research Center, Department of Food Sciences and Technology, Faculty of Nutrition and Food Sciences, Tabriz University of Medical Sciences, Tabriz, Iran. [3]Dental and Periodontal Research Center, Tabriz University of Medical Sciences, Tabriz, Iran. [4]Students' Scientific Research center, Food Safety and Hygiene Division, School of Public Health, Tehran University of Medical Sciences, Tehran, Iran. [5]Department of Food Sciences and Technology, Faculty of Nutrition and Food Sciences, Tabriz University of Medical Sciences, Tabriz, Iran. [6]Research Center for Environmental Determinants of Health (RCEDH), Kermanshah University of Medical Sciences, Kermanshah, Iran. [7]Food and Drug safety research center, Tabriz university of medical science, Tabriz, Iran. [8]Inorganic Chemistry Department, Faculty of Chemistry, University of Tabriz, C.P. 51664, Tabriz, Iran. *email: ehsani@tbzmed.ac.ir

were tested with an excellent antimicrobial activity in the efficient removal of pathogens. MONP may not show a considerable antimicrobial activity in form of metal oxide and metal salt alone, because of their tendency of aggregation[15]. However, the stability and slow release of metal ions from MONP are effective properties that can be tuned by appropriate synthesis. For this reason, new methods to immobilize MONP into zeolite membranes have been suggested[16]. One of the most important factors in antimicrobial activity is light. MONP, particularly ZnO and TiO_2, become activated against pathogenic bacteria when exposed to ultraviolet (UV) light[17,18]. The mechanism of this procedure involves substrate adsorption in the composite surface, depending on pH, temperature, composite stability, area and substrate concentration[19–22]. Some of the disadvantages are low adsorption ability (small active area) and photo corrosion[23,24]. Therefore, with precise preparation of ZnO and TiO_2, especially regarding morphologies and sizes, most of these caveats can be overcome[25–27].

MONP also show significant antimicrobial activity through connection to microbial DNA and proteins, and caused to preventing bacterial duplication, avoiding metabolic enzymes of the bacterial electron transport chain, leading to their inactivation[2].

The semiconductor properties of zinc oxide (ZnO) and titanium dioxide (TiO_2) can be tuned in nano scale[28–31]. Manufacturing nanoparticles involves protocols of different complexities with aggregation of ZnO and TiO_2 nanoparticles as an important limitation in the process[32,33]. These compounds are useful in pharmaceutical utilization[34], pigmentation[35], antimicrobial activities, anti-fungal and anti-viruses properties[36]. In addition, ZnO and TiO_2 are important components in the novel and active packaging industry.

Tiny ZnO and TiO_2 nanoparticles with a wide surface can maintain their photoactivity; however, their recovery at the end of the procedure is very difficult. Accordingly, a useful approach is to support ZnO and TiO_2 in a zeolite structure which can enhance adsorption and subsequently, increase the composite efficiency and ease of recovery by ordinary deposition[37,38]. The use of effective composites made up with ZnO and TiO_2 impregnated in zeolites is a new strategy to produces nanoparticles with supporter. Recent research reported some properties of ZnO supported in zeolites including ZSM-5, Y, X and A[39,40]. In this research, we have focused on the description and development of ZnO and TiO_2 nanoparticles supported in the channels of a porous matrix (4A zeolite) for antimicrobial application. First of all, we described a simple synthetic route for preparation of ZnO and TiO_2 impregnated into 4A zeolite (4A z). Secondly, the structural properties and antimicrobial effects of the materials were determined. In fact, zinc and titanium in high quantities may have toxic effects[41–45]; hence, in this work we have tried to use 4A z as a support of metal nanoparticles. These nanoparticles are encapsulated inside zeolite cavities or external channels to decrease the possibility of leaching as low as possible. This process reduces the toxicity of nanoparticles and their release from the matrix and therefore, this complex (nanoparticles and zeolite) can be used in polymer matrix for food packaging. In this work, we aimed to select the lowest effective amount of nanoparticles into 4A z with antimicrobial activity.

Materials and Methods

Materials. Here, 4A z ($Si/Al \cong 2$) was synthesized according to the formula below. Zinc acetate dehydrate, orthotitanate and ethanol were purchased from Merck. All the applied reagents were of analytical grade. It should be noted that in order to test antimicrobial activity, bacterial strains were obtained from Biological and Genetic Resource Center, Tehran, Iran. Nutrient broth and Nutrient agar were all purchased from Micromedia, Canada.

Measurements. X-ray diffraction patterns (XRD) were performed using a Siemens D5000 diffractometer with Cu kα radiation ($\lambda = 1.5418$ A and $2\theta = 4–70°$) at room temperature, 40 kV and 30 mA.

The degree of crystallinity is measured by peak height method[46] based on Eq. (1):

$$\text{Crystallinity Index(CrI)} = \left(\frac{I - I_0}{I}\right)100 \quad (1)$$

where CrI is crystallinity degree (%), I, is peak height at the angle of diffraction (2θ) related to crystalline section and I_0 is peak height at the angle of diffraction (2θ) related to non-crystalline section.

Scanning electron microscope (SEM) (Philips XL30) was evaluated to catch SEM images and to carry out elemental analysis. The SEM sample was gold coated prior to examination and SEM was operated at 5 kV. MAP was obtained by wavelength-dispersive X-Ray spectroscopy (WDS) system to show the spatial distribution of elements in a sample and be extremely useful for displaying element distributions in polymer matrix, particularly for showing compositional zonation. Transmission electron microscopy (TEM) was determined by electrons microscope systems and was also used to indicate the interactions between the electrons and the atoms in order to observe crystal structure and features in the structure like dislocations and grain boundaries. The minimum inhibitory concentration (MIC_{90}), minimum bactericidal concentration (MBC) and fractional inhibitory concentration (FIC) of MONP dropped into 4A z were also determined.

Methods

Preparation of 4A zeolite. 4A z (alumina silicates) with a silica to alumina ratio ($Si/Al \cong 2$) was synthesized by hydrothermal method. In this process, clinoptilolite and alumina were used as sources of silicon and aluminum, respectively, and then mixed with NaOH. In the final stage, the solution was conveyed to teflon reactor at 90 °C, in order to produce 4A z nanocomposite[37].

Preparation of ZnO doped into 4A zeolite. In this research, ZnO clusters were synthesized by the following stage response: in the first step, a solution of 0.17 g $Zn(CH_3CHOO)_2{\cdot}2H_2O$ was prepared, mixed with a ratio of 5:95% w/w (nanoparticles:4A z) and was shaken for 30 min. In the second step, integration of zinc acetate to 4A z using an ion exchange process was done (24 h at 60 °C). Next, by the use of distilled water, the solution was washed and dried at 80 °C. The final powder was calcined at 500 °C for 2 h to produce ZnO/4A z nanocomposite.

Preparation of TiO_2 doped into the 4A zeolite. In this research TiO_2 salt was created by the following stage response: in the first step, 0.2 g ortho titanate was dissolved in ethanol. Then, this solution was mixed with a ratio of 5:95% w/w (nanoparticles:4A z) and was shaken for 30 min. In the second step, integration of ortho titanate to 4A z using an ion exchange process was done (6 h at 90 °C). Next, by the use of distilled water, the solution was washed and dried at 80 °C. The final powder was calcined at 500 °C for 2 h in order to produce TiO_2/4A z nanocomposite.

Preparation of ZnO and TiO_2 doped into 4A zeolite. In order to prepare ZnO/TiO_2doped into 4A z, ZnO nanoparticle was prepared and mixed with a ratio of 2.5:95% w/w (nanoparticles:4A z). Then, 2.5% w/w titanium dioxide ethanol dried powder was added to the mixture of 4A z and ZnO and dried at 80 °C. The final powder was calcined at 500 °C for 2 h in order to produce TiO_2 and ZnO/4A z nanocomposite.

Determination of minimum inhibitory concentration (MIC), minimum bactericidal concentration(MBC) and fractional inhibitory concentration (FIC). The antimicrobial activity of 4A z, TiO2/4A z, and ZnO/4A z was defined by micro dilution method on 96-well microplates according to previously reported methods (Tajik *et al*., 2015). Four bacterial suspensions including *Escherichia coli* O157:H7 (IBRC-M 10698), *Listeria monocytogenes* (IBRC-M 10671), *Pseudomonas fluorescens* (IBRC-M 10752), and *Staphylococcus aureus* (IBRC-M 10690) were collected after 24 h cultures on Nutrient broth and regulated to 0.5 McFarland standard turbidity (1.5×10^{-8} CFU/mL). In order to evaluating antimicrobial activity of nanoparticles, we used bacterial suspensions (20 µL), different concentrations of 4A z, TiO2/4A z, ZnO/4A z and TiO_2, ZnO/4A z suspension (0.5, 1, 2, 3, 4, 5, 6 and 7 mg/mL), 20 µL for each nanoparticles or 4A z and 10 µL in combination; and 160 µL of Nutrient broth in tested wells. The last wells of micro-plates were considered as positive controls containing uninoculated broth with antimicrobials materials (nanoparticles), and as negative controls containing inoculated broth without antimicrobials materials. The microplates were incubated at 37 °C for 24 h under constant shaking (50–100 rpm) by a microplate shaker (Boeco, Hamburg, Germany). It should be noted that for *Pseudomonas fluorescens*, we needed 25 °C for 24 h. MIC_{90} values were determined as the lowest concentration with no visible bacterial growth. The best concentration of each antimicrobial agent was determined by MIC method.

The MBC is the lowest concentration of an antibacterial agent required to kill a particular bacterium[47,48]. It can be determined from broth dilution MIC tests by sub culturing to agar plates that do not contain the test agent. The minimum bactericidal concentration is identified by determining the lowest concentration of antibacterial agent that reduces the viability of the initial bacterial inoculum by $\geq$99.9%. The MBC is complementary to MIC; whereas, MIC test demonstrates the lowest level of antimicrobial agent that inhibits growth, MBC test demonstrates the lowest level of antimicrobial agent that results in microbial death[49,50]. The fractional inhibitory concentration was used for combination of materials based on the following equation:

$$FIC_{A\&B} = \frac{MIC(A\&B)}{MIC(A) + MIC(B)}$$

where A refers to TiO_2 nanoparticles and B refers to ZnO nanoparticles.

Determination of antibacterial activity of nanoparticles doped in 4Azeolite. The disc diffusion test was performed to determine the antibacterial activity of nanoparticles doped in 4A z[51]. *Pseudomonas fluorescens*, *Staphylococcus aureus*, *Listeria monocytogenes*, and *Escherichia coli* O_{157}:H_7 suspensions were collected from 18 h nutrient broth cultures then adjusted to 0.5 McFarland standard turbidity (1.5×10^{-8} CFU/mL) and diluted (1:10) to the desired bacterial density (1.5×10^{-6} CFU/mL). The Mueller-Hinton agar medium was then inoculated with 0.1 mL of the bacterial suspensions (1.5×10^{-6} CFU/mL). Next, the suspensions of nanoparticles doped in 4A z and also 4A z individually, were prepared under sterile conditions and then situated on the surface of Mueller-Hinton agar plates (100 λ). The plates were incubated at 37 °C (for *L. monocytogenes*, *E. coli* O_{157}:H_7, and *S. aureus*) or 25 °C (for *P. fluorescens*) for 24 h, after which the inhibition zone around the discs were measured by a digital micrometer. Indeed, inhibition zone have shown the antibacterial effect of nanoparticles. The greater the diameter of the inhibitory zone, the greater antimicrobial activities of nanoparticles.

Inductively coupled plasma mass spectroscopy (ICP-MS). Migration tests were performed according to EU regulation for plastic materials and articles intended to be in contact with food (Regulation 10/2011/EU)[52]. Migration of TiO_2 and ZnO nanoparticles was assessed using a simulant (deionized water with pH = 6–7) over 12 days at 25–30 °C. Prior to the migration tests, the concentration of ZnO and TiO_2 nanoparticles in 4A z was determined. In ICP-MASS assay, we first produced a nano bio-composite film with selected polymer and nanoparticles zeolite. Then, this nano bio-composite film was converted to food packaging by thermal processing. Next, to measure the migration of nanoparticles zeolite from food packaging to food product, we have used food simulant. Food simulant was filled in food packaging, packed and stored for 12 days. Next, the simulants were filtered through a 220 nm Millipore filter and then migrated nanoparticles were analyzed using ICP-MS (Agilent 7800 Quadrupole ICP-MS, Perkin Elmer, California, United States). In the final stage, the migration results were normalized to nanoparticles migrated/cm^2 after 12 days. It should be noted that, on the first day, the measurement of nanoparticles zeolite in food packaging was conducted regardless of food simulant. This was to discover the exact amount of nanoparticles embedded in 4A z and polymer matrix.

Ethical approval. This article does not contain any studies with human participants or animals performed by any of the authors.

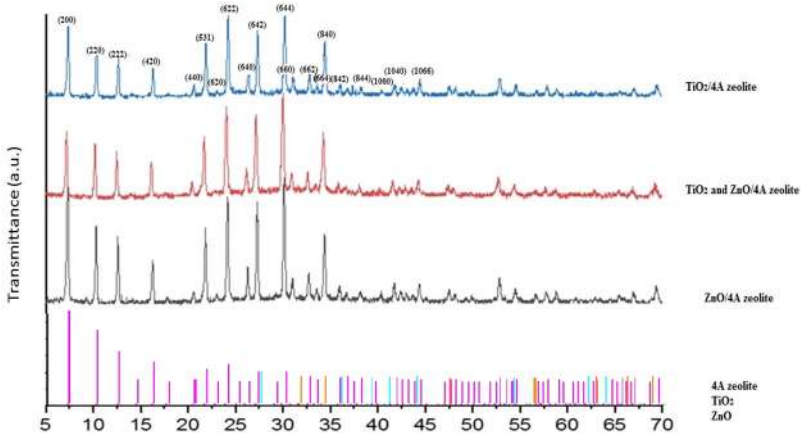

Figure 1. XRD spectra of nanocomposite TiO_2/4A z, TiO_2, ZnO/4Az and ZnO/4A z. Pink color is 4A z individually, blue color is TiO_2 nanoparticle individually and orange color is ZnO nanoparticle individually.

Results and Discussion

Evaluation of XRD patterns. XRD showed the impact of homogenization on crystalline structure of the combination[53,54]. XRD patterns of ZnO, TiO_2, and ZnO/TiO_2 supported into 4A z are shown in Fig. 1. Based on the obtained template, TiO_2 nanoparticles in the form of anatase, had significant peaks at $2\theta = 7.36$, 10.31, 12.66, 21.90, 24.21,27.32,30.14, 30.19 and 34.41°. According to Scherrer equation ($\tau = \kappa\ \lambda/\beta\ \cos\theta$), the average crystallite size of nanoparticle was approximated to be 50 nm. In this equation, τ is the average crystalline size, κ is the shape factor (about 0.9), λ is the wavelength of X-ray radiation, β is the full wide at half the maximum intensity and θ is the Bragg diffraction angle[55]. As shown in Fig. 1, the peaks of 4A z are visible at certain 2θ with high intensity. The diffraction peaks for ZnO and TiO_2 were in good agreement with those given in the standard data (PCPDF, 79–0207 and JCPDS, 21–1272, respectively) with acceptable crystallinity. According to XRD patterns, it was found that ZnO and TiO_2 was crystallized with hexagonal wortzite and anatase phase, respectively. On the other hand, it is clear to see that the width of the reflections is considerably broadened, which indicates a small crystalline domain size. In the spectra of oxide nanoparticles doped into 4A z, the presence of nanoparticles can be confirmed based on the observed peaks, in particular $2\theta = 4$–70. Regarding the significant peaks with miller indices of TiO_2(642), (664) and ZnO (842), (664), they have considerable overlap with the peaks of 4A z (Fig. 1), and therefore, the oxide nanoparticle peaks are not clearly visible.

But according to MAP pattern, the presence of elements (titanium and zinc) has been confirmed which affects the intensity of 4A z peaks (Fig. 2). Also, it should be noted that in ZnO/TiO_2 spectrum, the intensity of crystalline plates with Miller indices (200, 220 and 222) are lower than when there is only one type of metal oxide.

Evaluation of SEM, TEM and MAP patterns. The size and morphology of the samples are illustrated in Fig. 2(A–C). According to Figs. 2A, 3A z particles with cubic structure are completely visible and ZnO and TiO_2 nanoparticles are dispersed in the form of almost spherical particles into 4A z. Based on Fig. 2A, cube-shaped particles are completely apart from one another and the deformed structures are not visible. The image (Fig. 2A) showed that the matrix of ZnO and TiO_2 nanoparticles had homogeneous and smooth surfaces without any roughness and cracks, which indicated proper synthesis of the materials. The size of 4A z particles, based on Fig. 2A,B, is 400 to 600 nm; besides the oxide nanoparticles are very thin and smaller than 50 nm. According to the obtained images (Fig. 2B,C), the dispersion of ZnO and TiO_2 nanoparticles into 4A z structure is uniform and no accumulation has been observed. Also, cubic particles with square layers are present. Figure 2B shows a typical TEM micrograph of ZnO/TiO_2 nanoparticles powder. This powder is formed by 10–50 nm size particles having equiaxed morphology. The particles are well separated from each other. Dark field imaging displayed that each particle was a single crystal. The nanoparticle sizes from TEM examination were in good agreement with both XRD and MAP.

MIC, MBC and FIC values of nanoparticles. MIC_{90}, MBC and FIC values of 4A z, TiO_2/4A z, ZnO/4A z, and TiO_2, ZnO/4A z nanocomposite are shown in Tables 1–3. And 4A z do not have antimicrobial activity against bacteria's[56] (Table 1). TiO_2/4A z, ZnO/4A z, and TiO_2/ZnO/4A z nanocomposite were activated in the concentrations of 1–4 mg/mL against *E. coliO*157:*H7, S. aureus, P. fluorescens*, and *L. Monocytogenes*, separately. These results were in agreement with the outcome of prior studies[57,58]. The best concentrations of MIC were selected for TiO_2/4A z, ZnO/4A z, and TiO_2, ZnO/4A z nanocomposite as 2, 1 and 1 mg/mL, respectively; against microorganisms (Table 1). This concentration in MBC corresponded to 2, 2 and 2 mg/mL, respectively; and 0.25 mg/ml concentration of TiO_2, ZnO/4A z nanocomposite against *E. coli* O_{157}:H_7, had an excellent FIC value (Table 3). Based on the results, gram negative bacteria were more sensitive compared to antimicrobial agents. Gram positive bacteria have a thick layer of peptidoglycan in their cell walls which have caused more resistance compared to gram negative bacteria against antimicrobial agent. Gram negative bacteria contains a thin peptidoglycan layer which facilitates the mobility of metal ion nanoparticles to the cell, and it also assists the interaction between nanoparticle and bacterial cell walls due to lack of thick peptidoglycan layer. Another aspect of gram negative

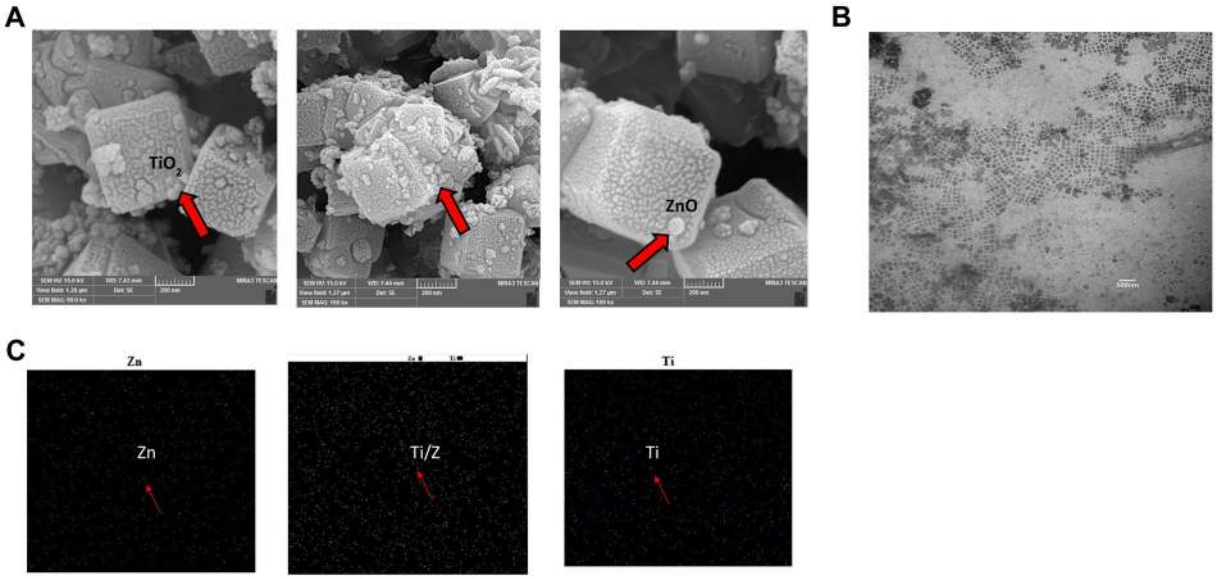

Figure 2. (**A**) Evaluation of SEM pattern; a: ZnO/4A z, b: TiO_2, ZnO/4A z and c: TiO_2/4A z. (**B**) Evaluation of TEM image; a: TiO_2 and ZnO/4A z. (**C**) Evaluation of MAP images; a: ZnO/4A z, b: TiO_2, ZnO/4A z and c: TiO_2/4A z.

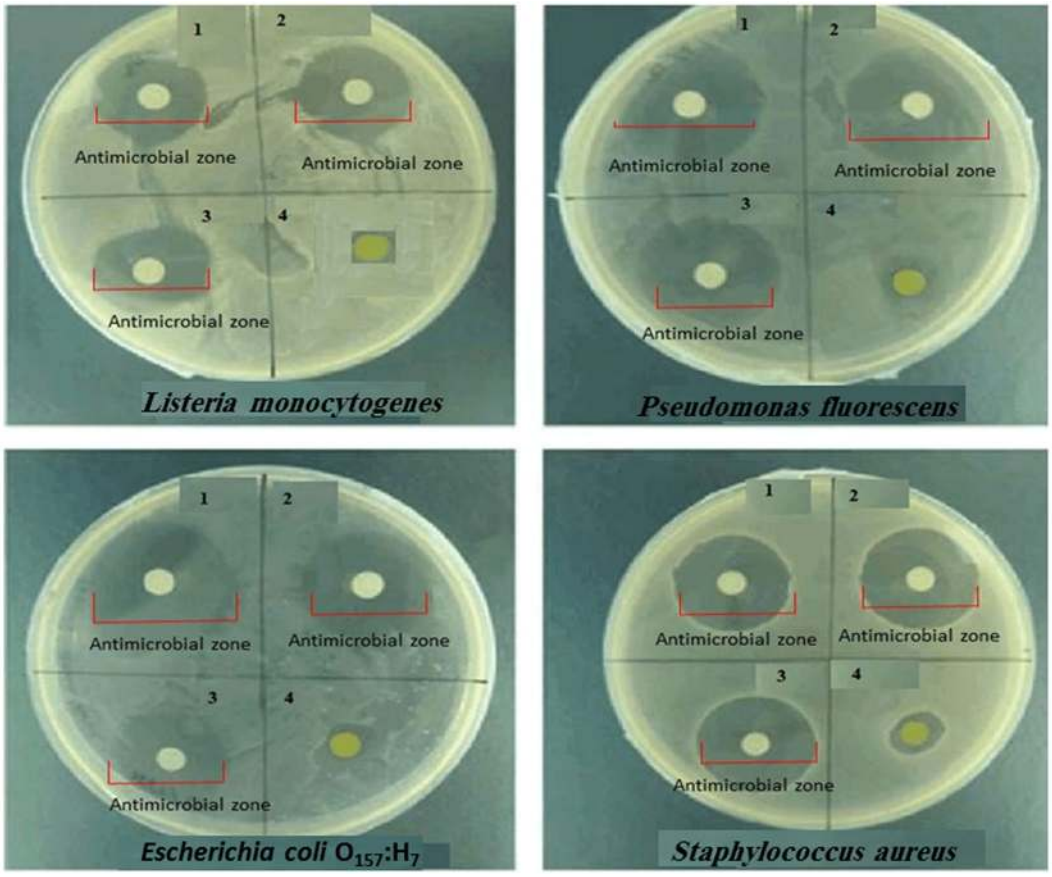

Figure 3. Disc diffusion test of nanoparticles doped in 4A z. In each figure: number 1 is ZnO/4A z, number 2 is TiO_2/4A z, number 3 is ZnO and TiO_2/4A z and number 4 is 4A z.

bacteria is the negative charge of lipopolysaccharide layer. This charge has a role as a significant incorporation factor for positive ions, which consequently leads to nanoparticle emission, intracellular damages and destruction of DNA and proteins (Fig. 4).

Bacteria	MIC_{90} (mg/ml)			
	4A z	TiO_2/4A z	ZnO/4A z	TiO_2/ZnO/4A
E. coli O157:H7	0	2 ± 0.01	2 ± 0.02	1 ± 0.01
S. aureus	0	3 ± 0.01	3 ± 0.02	2 ± 0.01
P. fluorescens	0	2 ± 0.01	1 ± 0.01	1 ± 0.01
L. Monocytogenes	0	3 ± 0.01	2 ± 0.00	2 ± 0.01

Table 1. MIC of TiO_2, ZnO, and TiO_2 and ZnO doped in 4A z against bacteria. MIC: Minimum Inhibition ConcentrationTiO_2: Titanium dioxide, ZnO: Zinc oxide, 4A z: 4A zeolite.

Bacteria	MBC (mg/ml)			
	4A z	TiO_2/4A z	ZnO/4A z	TiO_2/ZnO/4A z
E. coli O157:H7	0	2 ± 0.01	3 ± 0.02	2 ± 0.01
S. aureus	0	4 ± 0.01	4 ± 0.01	3 ± 0.01
P. fluorescens	0	3 ± 0.01	2 ± 0.01	2 ± 0.01
L. Monocytogenes	0	4 ± 0.02	3 ± 0.00	3 ± 0.01

Table 2. MBC of TiO_2, ZnO, and TiO_2 and ZnO doped in 4A z against bacteria. MBC: Minimum bactericidal ConcentrationTiO_2: Titanium dioxide, ZnO: Zinc oxide,4A z: 4A zeolite.

Bacteria	FIC (mg/ml)
	TiO_2/ZnO/4A z
E. coli O157:H7	0.25 ± 0.01
S. aureus	0.33 ± 0.01
P. fluorescens	0.33 ± 0.01
L. Monocytogenes	0.40 ± 0.01

Table 3. FIC of TiO_2/ZnO doped in 4A z against bacteria. FIC: fractional inhibitory concentration TiO_2: Titanium dioxide ZnO: Zinc oxide, 4A z: 4A zeolite.

Bacteria strains	Control sample	Inhibition zone (mm)		
		Treatment 1	Treatment 2	Treatment 3
L. monocytogene	0	6.25 ± 0.02 a	8.82 ± 0.03 e	9.51 ± 0.01 i
E. coli $O_{157}H_7$	0	6.86 ± 0.03 b	9.13 ± 0.03 f	10.73 ± 0.04 j
S. aureus	0	6.21 ± 0.02 c	7.58 ± 0.6 g	9.22 ± 0.02 k
P. fluorescens	0	6.34 ± 0.03 d	8.97 ± 0.04 h	9.85 ± 0.01 l

Table 4. Disc diffusion analysis of nanoparticles doped in 4A z. Control sample: Zeolite 4A, Treatment 1: ZnO/4A z, Treatment 2: TiO_2/4A z, and Treatment 3: ZnO and TiO_2/4A z. Date are presented as mean ± SD and analyzed with one-way analysis of variance. Different letters represent statistical significance among different treatment using the Tukey.

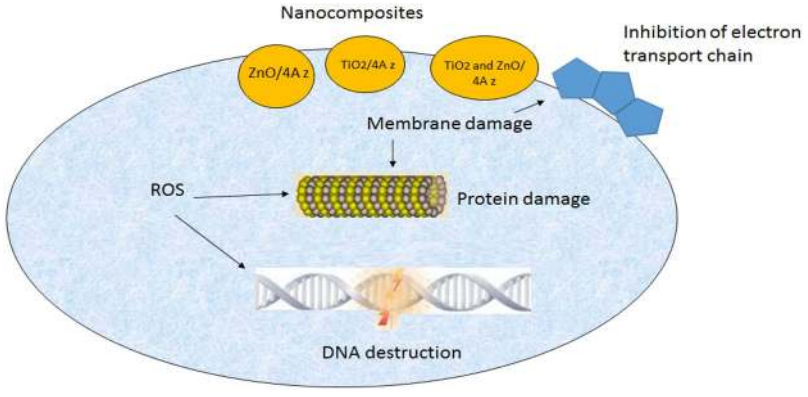

Figure 4. Antimicrobial mechanism of nanocomposites (TiO_2/4A z, ZnO/4A z and TiO_2 and ZnO/4A z).

Nanoparticles zeolite Migration rate (ppb)	ZnO/4A z	TiO_2/4A z	ZnO and TiO_2/4A z
Frist day	1031	655	1259
Twelfth day	943.3	3.1	344.1

Table 5. Migration assay of nanoparticles zeolite with ICP-MASS test.

Antibacterial activity of nanoparticles doped in 4A zeolite. The disc diffusion procedure was conducted to assess the antimicrobial activity of nanoparticles doped in 4A z (Table 4). Inhibition zone diameter indicated that TiO_2, ZnO/4A z had a greater antimicrobial effect against bacteria compared to the combination of individual nanoparticles with 4A z (Fig. 3). Also it should be noted that, 4A z individually do not have an antimicrobial activity against bacteria[56]. Based on the results, Gram-negative bacteria (particularly *E. coli* $O_{157}H_7$) were more sensitive to the antimicrobial agents. The main purpose of using 4A z, as a carrier with nanoparticles, is to control the release of them and increase the antimicrobial activity. The highest zone of inhibition was seen against *E. coli* $O_{157}H_7$ including, 6.86 ± 0.03 mm, 9.13 ± 0.03 mm, and 10.73 ± 0.04 mm for ZnO/4A z, TiO_2/4A z and ZnO and TiO_2/4A z, respectively; while *S. aureus* had the lowest inhibitory zone in all treatments ($P < 0.05$). Indeed, nanoparticles disturb the permeability of both the cell wall and cell membrane, thereby affect biomolecules such as DNA and protein, and prevent processes such as DNA replication and protein synthesis[59].

Titanium dioxide (TiO_2), is also called titania, is one of the most widely used semiconductor nanoparticles with specific hydrophilic and photocatalytic properties, which caused to antimicrobial and ultraviolet (UV) protecting characteristics[51,60]. These nanoparticles are extensively used in producing polymer nanocomposites in food packaging. TiO_2 nanoparticle works in two phases: first, the ability to degrade bio polymeric compound (such as polysaccharides and proteins)[61] on its surface and second, to alter the surface properties of the objects to hydrophilic state when TiO_2 is placed on that surface. In Europe, TiO_2 (E171) is confirmed and categorized as a color additive in confectionaries, dairy products, and soft drinks under Directive of 1994/36/EC[62]. TiO_2 is more prone to oxidization when exposed to ultraviolet (UV) in a wavelength lower than 385 nm. As a result, TiO_2 can produce active oxygen species when exposed to sunlight[63]. Furthermore, the antimicrobial activity of TiO_2 is related to its crystal structure, the kind of artificial light, UVA light intensity, shape and size[64] as well as production of ROS, active radical species, hydrogen peroxide, superoxide radical, and hydroxyl radical[64–66]. These active species destroy the outer membrane of the bacteria, namely phospholipids, proteins and lipopolysaccharides and finally damage the bacteria.

ZnO is recognized as a colorless, wide band gap semiconductor with an optical band gap in UV region which makes it applicable as an impressive absorbent of UV radiation. Currently, ZnO is listed as generally recognized as safe (GRAS) by the US Food and Drug Administration (FDA) and is consumed as a food additive, considering the fact that zinc is an important trace element in nutrition[67]. The antimicrobial activities and potential applications of ZnO nanoparticles in food preservation have been approved[68]. In this regard, ZnO nanoparticles were combined in polymeric matrix in order to supply the packaging material with antimicrobial activity and to improve some packaging properties[69,70]. Furthermore, the antimicrobial properties of ZnO is related to photocatalytic activity of H_2O_2. Both Zn^{+2} and ZnO particles hold antibacterial activities. The antimicrobial activities of ZnO at nanoscale would yield affordable and safe innovative strategies[69,71]. Moreover, ZnO has been blended into the linings of food cans used for meat, fish, corn, and peas to preserve colors and hinder spoilage because of its antimicrobial action.

Indeed nanoparticles have the ability to decline or remove the microorganism resistance by two mechanisms: (a) free metal ion toxicity arising from dissolution of metals from the surface of nanoparticles and (b) oxidative stress via generation of reactive oxygen species (ROS) using hydrogen peroxide (H_2O_2) and organic hydro peroxides (OHP) on the surface of nanoparticles[72]. Actually, nanoparticle can effect on the survival of microorganisms by agglomeration on the surface of bacteria and alter the structure of lipids, peptidoglycan, proteins and their DNA[73]. But there may be differences in the impact of nanoparticles on types of specific microorganisms; for instance, Sierra *et al.*[74] showed a higher antimicrobial effect against *Streptococcus mutans* of Cu nanoparticles at lower concentrations than zinc. In another study, Ruparelia *et al.*[75] showed that copper nanoparticle has great impact as an antimicrobial agent against *E. coli*, *Bacillus subtilis*, and *Staphylococcus aureus* in comparison with TiO_2. Our results are in agreement with those of Lou *et al.*[59] and Yael N *et al.*[76].

Inductively coupled plasma mass spectroscopy. Migration is a mass transfer process where low molecular mass particles are released into the surroundings. To assess migration, the system must be simplified and particles must be analyzed separately. The package is assumed to be homogeneous, the food is substituted by food simulants and the substance is introduced at the recognized concentration. In this research, nanoparticles ion releasing capacity in food simulants of the composites was quantified by ICPMASS.

Zinc and Titania ions are doped into 4A z through ionic exchange, preferably with Na^+ ions[77]. Next, ions are released from composites through ionic exchange with cations/protons present in food simulants, and their concentration determines the amount of released nanoparticles. Therefore, for applications where a long-term antibacterial activity is expected, nanoparticles zeolites should be placed in solutions with low ionic strength[78]. The immersion of matrix (nanoparticles doped in 4A z) in distilled water (as a food simulant) demonstrated that nanoparticles were sensitive to water. When the matrix was immersed in water for a long period of time, the water molecules interacted with polar groups in nanoparticles were doped in 4A z, which led to the swelling and deformation of the matrix. According to ICP-MS results (Table 5), the amount of ZnO in ZnO/4A z was initially 1031

ppb, and decreased to 943.3 ppb (ZnO/4A z) after 12 days of immersion in food simulant. These values were 655 and 3.1 ppb for TiO_2/4A z, respectively; while they were recorded to be 1259 and 344.1 ppb for ZnO and TiO_2/4A z. Based on the results, the migration values for ZnO, TiO_2, and ZnO and TiO_2 were approximately 47%, 0.47% and 21%, respectively. It is worth mentioning that ZnO and TiO_2 have been approved by the US Food and Drug Administration (FDA) as safe compounds to be used in food and food contact materials at restricted quantities below 2 and 1% of the food weight for ZnO and TiO_2 nanoparticles, respectively[79,80]. Moreover, low amounts of ZnO and TiO_2 nanoparticles are beneficial for the human body because of their antimicrobial and anticancer properties. ICP-MS was used to detect the metal ions with high sensitivity, and it could detect very low signals of ZnO and TiO_2 nanoparticles from the digested solutions. These results revealed that the slight migration of nanoparticles occurs in food simulant; however,this amount is in accordance with the standard rate by FDA[81]. Our results regarding TiO_2 nanoparticles are in accordance with those of Lian *et al*.[82].

Conclusions

TiO_2, ZnO and TiO_2/ZnO nanoparticles supported into 4A z were successfully synthesized through hydrothermal method, and were evaluated for antimicrobial activity for the first time. The size of 4A z particles were around 400 to 600 nm and the average crystallite size of nanoparticles was approximately 50 nm. The XRD, SEM, MAP and TEM analysis demonstrated that crystallographic plate, size, shape and morphology of nanocomposite (nanoparticles with 4A z) are very close to 4A z itself. Moreover, the results of antimicrobial test confirmed a considerable antimicrobial activity against gram positive and negative bacteria of the nanoparticles supported in 4A z. Indeed, the antimicrobial activity of nanoparticles embedded into 4A z was dependent on the type of nanoparticles and on the species of microorganism (gram positive or gram negative). The most sensitive bacteria were *P. fluorescens* and then *E. coli* O157:H7. Embedding of nanoparticles in 4A z caused to control the release of them, and enhance their antimicrobial properties. Hence, using these composites can be a promising approach to create new active packaging in food industry.

Received: 26 June 2019; Accepted: 16 October 2019;
Published online: 25 November 2019

References

1. Davis, M. E. Ordered porous materials for emerging applications. *Nature* **417**, 813 (2002).
2. Holt, K. B. & Bard, A. J. Interaction of silver (I) ions with the respiratory chain of Escherichia coli: an electrochemical and scanning electrochemical microscopy study of the antimicrobial mechanism of micromolar Ag+. *Biochemistry* **44**, 13214–13223 (2005).
3. Hrenovic, J., Milenkovic, J., Daneu, N., Kepcija, R. M. & Rajic, N. Antimicrobial activity of metal oxide nanoparticles supported onto natural clinoptilolite. *Chemosphere* **88**, 1103–1107 (2012).
4. Lu, J. *et al*. Coking-and sintering-resistant palladium catalysts achieved through atomic layer deposition. *Science* **335**, 1205–1208 (2012).
5. Radnik, J. *et al*. Deactivation of Pd acetoxylation catalysts: Direct observations by XPS investigations. *Angewandte Chemie International Edition* **44**, 6771–6774 (2005).
6. Baker, L. R. *et al*. Furfuraldehyde hydrogenation on titanium oxide-supported platinum nanoparticles studied by sum frequency generation vibrational spectroscopy: acid–base catalysis explains the molecular origin of strong metal–support interactions. *Journal of the American Chemical Society* **134**, 14208–14216 (2012).
7. Liu, X. *et al*. Strong metal–support interactions between gold nanoparticles and ZnO nanorods in CO oxidation. *Journal of the American Chemical Society* **134**, 10251–10258 (2012).
8. Garcia, La, French, R., Czernik, S. & Chornet, E. Catalytic steam reforming of bio-oils for the production of hydrogen: effects of catalyst composition. *Applied Catalysis A: General* **201**, 225–239 (2000).
9. Yin, A.-X., Min, X.-Q., Zhang, Y.-W. & Yan, C.-H. Shape-selective synthesis and facet-dependent enhanced electrocatalytic activity and durability of monodisperse sub-10 nm Pt− Pd tetrahedrons and cubes. *Journal of the American Chemical Society* **133**, 3816–3819 (2011).
10. Arribas, M. & Martınez, A. The influence of zeolite acidity for the coupled hydrogenation and ring opening of 1-methylnaphthalene on Pt/USY catalysts. *Applied. Catalysis A: General* **230**, 203–217 (2002).
11. Wang, L. *et al*. Mesoporous ZSM-5 zeolite-supported Ru nanoparticles as highly efficient catalysts for upgrading phenolic biomolecules. *ACS Catalysis* **5**, 2727–2734 (2015).
12. Wang, C. *et al*. Product selectivity controlled by zeolite crystals in biomass hydrogenation over a palladium catalyst. *Journal of the American Chemical Society* **138**, 7880–7883 (2016).
13. Wang, L., Xu, S., He, S. & Xiao, F.-S. Rational construction of metal nanoparticles fixed in zeolite crystals as highly efficient heterogeneous catalysts. *Nano Today* (2018).
14. Marshall, M. M., Naumovitz, D., Ortega, Y. & Sterling, C. R. Waterborne protozoan pathogens. *Clinical microbiology reviews* **10**, 67–85 (1997).
15. Heinlaan, M., Ivask, A., Blinova, I., Dubourguier, H.-C. & Kahru, A. Toxicity of nanosized and bulk ZnO, CuO and TiO2 to bacteria Vibrio fischeri and crustaceans Daphnia magna and Thamnocephalus platyurus. *Chemosphere* **71**, 1308–1316 (2008).
16. Sabbani, S. *et al*. Synthesis of silver-zeolite films on micropatterned porous alumina and its application as an antimicrobial substrate. *Microporous and Mesoporous Materials* **135**, 131–136 (2010).
17. Adams, L. K., Lyon, D. Y. & Alvarez, P. J. Comparative eco-toxicity of nanoscale TiO2, SiO2, and ZnO water suspensions. *Water research* **40**, 3527–3532 (2006).
18. Ravishankar Rai, V. & Jamuna Bai, A. Nanoparticles and their potential application as antimicrobials. *A Méndez-Vilas A, editor. Mysore: Formatex* (2011).
19. Herrmann, J.-M. Photocatalysis fundamentals revisited to avoid several misconceptions. *Applied Catalysis B: Environmental* **99**, 461–468 (2010).
20. Akpan, U. G. & Hameed, B. H. Parameters affecting the photocatalytic degradation of dyes using TiO2-based photocatalysts: a review. *Journal of hazardous materials* **170**, 520–529 (2009).
21. Chong, M. N., Jin, B., Chow, C. W. & Saint, C. Recent developments in photocatalytic water treatment technology: a review. *Water research* **44**, 2997–3027 (2010).
22. Zhang, L., Mohamed, H. H., Dillert, R. & Bahnemann, D. Kinetics and mechanisms of charge transfer processes in photocatalytic systems: a review. *Journal of Photochemistry and Photobiology C: Photochemistry Reviews* **13**, 263–276 (2012).

23. Lee, K. M., Lai, C. W., Ngai, K. S. & Juan, J. C. Recent developments of zinc oxide based photocatalyst in water treatment technology: a review. *Water research* **88**, 428–448 (2016).
24. Kalinauskas, P., Valsiūnas, I. & Juzeliūnas, E. Zinc photo-corrosion in neutral solutions. *Corrosion science* **43**, 2083–2092 (2001).
25. Dong, X. *et al*. Morphology evolution of one-dimensional ZnO nanostructures towards enhanced photocatalysis performance. *Ceramics International* **42**, 518–526 (2016).
26. Gnanaprakasam, A., Sivakumar, V., Sivayogavalli, P. & Thirumarimurugan, M. Characterization of TiO2 and ZnO nanoparticles and their applications in photocatalytic degradation of azodyes. *Ecotoxicology and environmental safety* **121**, 121–125 (2015).
27. Azizi-Lalabadi, M. *et al*. Nanoparticles and zeolites: Antibacterial effects and their mechanism against pathogens. *Current pharmaceutical biotechnology* (2019).
28. Geetha, N. *et al*. High Performance Photo-Catalyst Based on Nanosized ZnO–TiO2 Nanoplatelets for Removal of RhB Under Visible Light Irradiation. *Journal of Advanced Microscopy Research* **13**, 12–19 (2018).
29. Evgenidou, E., Fytianos, K. & Poulios, I. Semiconductor-sensitized photodegradation of dichlorvos in water using TiO2 and ZnO as catalysts. *Applied Catalysis B: Environmental* **59**, 81–89 (2005).
30. Brus, L. E. Electron–electron and electron-hole interactions in small semiconductor crystallites: The size dependence of the lowest excited electronic state. *The Journal of chemical physics* **80**, 4403–4409 (1984).
31. Fang, J. *et al*. Stability of co-existing ZnO and TiO2 nanomaterials in natural water: Aggregation and sedimentation mechanisms. *Chemosphere* **184**, 1125–1133 (2017).
32. Zhang, J. *et al*. Solvent-Free Synthesis of Zeolite Crystals Encapsulating Gold–Palladium Nanoparticles for the Selective Oxidation of Bioethanol. *ChemSusChem* **8**, 2867–2871 (2015).
33. Kołodziejczak-Radzimska, A. & Jesionowski, T. Zinc oxide—from synthesis to application: a review. *Materials* **7**, 2833–2881 (2014).
34. Bhuyan, T., Mishra, K., Khanuja, M., Prasad, R. & Varma, A. Biosynthesis of zinc oxide nanoparticles from Azadirachta indica for antibacterial and photocatalytic applications. *Materials Science in Semiconductor Processing* **32**, 55–61 (2015).
35. Kiomarsipour, N., Razavi, R. S., Ghani, K. & Kioumarsipour, M. Evaluation of shape and size effects on optical properties of ZnO pigment. *Applied Surface Science* **270**, 33–38 (2013).
36. Janaki, A. C., Sailatha, E. & Gunasekaran, S. Synthesis, characteristics and antimicrobial activity of ZnO nanoparticles. *Spectrochimica Acta Part A: Molecular and Biomolecular Spectroscopy* **144**, 17–22 (2015).
37. Khatamian, M., Divband, B. & Jodaei, A. Degradation of 4-nitrophenol (4-NP) using ZnO nanoparticles supported on zeolites and modeling of experimental results by artificial neural networks. *Materials Chemistry and Physics* **134**, 31–37 (2012).
38. Guo, Y., Zu, B. & Dou, X. Zeolite-based photocatalysts: a promising strategy for efficient photocatalysis. *Journal of Thermodynamics & Catalysis* **4**, 1 (2013).
39. Tekin, R., Erdogmus, H. & Bac, N. Assessment of Zeolites as Antimicrobial Fragrance Carriers (2017).
40. Ferreira, L., Fonseca, A. M., Botelho, G., Almeida-Aguiar, C. & Neves, I. C. Antimicrobial activity of faujasite zeolites doped with silver. *Microporous and Mesoporous Materials* **160**, 126–132 (2012).
41. Federici, G., Shaw, B. J. & Handy, R. D. Toxicity of titanium dioxide nanoparticles to rainbow trout (Oncorhynchus mykiss): Gill injury, oxidative stress, and other physiological effects. *Aquatic toxicology* **84**, 415–430 (2007).
42. Cupi, D., Hartmann, N. B. & Baun, A. The influence of natural organic matter and aging on suspension stability in guideline toxicity testing of silver, zinc oxide, and titanium dioxide nanoparticles with Daphnia magna. *Environmental toxicology and chemistry* **34**, 497–506 (2015).
43. Cox, A., Venkatachalam, P., Sahi, S. & Sharma, N. Reprint of: silver and titanium dioxide nanoparticle toxicity in plants: a review of current research. *Plant physiology and biochemistry* **110**, 33–49 (2017).
44. Yin, Y. *et al*. Elevated CO 2 levels increase the toxicity of ZnO nanoparticles to goldfish (Carassius auratus) in a water-sediment ecosystem. *Journal of hazardous materials* **327**, 64–70 (2017).
45. Langston, W. In *Heavy metals in the marine environment* 101–120 (CRC Press, 2017).
46. Segal, L., Creely, J., Martin, A. Jr. & Conrad, C. An empirical method for estimating the degree of crystallinity of native cellulose using the X-ray diffractometer. *Textile Research Journal* **29**, 786–794 (1959).
47. Krishnan, R., Arumugam, V. & Vasaviah, S. K. The MIC and MBC of Silver Nanoparticles against Enterococcus faecalis-A Facultative Anaerobe. *J Nanomed Nanotechnol* **6**, 285 (2015).
48. Qi, L., Xu, Z., Jiang, X., Hu, C. & Zou, X. Preparation and antibacterial activity of chitosan nanoparticles. *Carbohydrate research* **339**, 2693–2700 (2004).
49. Venegas, M. A. *et al*. Nanoparticles against resistant Pseudomonas spp. *Microbial pathogenesis* **118**, 115–117 (2018).
50. Abdollahzadeh, E. The qualitative and quantitative antibacterial activity of cinnamon essential oil (Cinnamomum zeylanicum) and ZnO nanoparticles against Listeria monocytogenes. *Fisheries Science and Technology* **7**, 49–55 (2018).
51. Sani, M. A., Ehsani, A. & Hashemi, M. Whey protein isolate/cellulose nanofibre/TiO2 nanoparticle/rosemary essential oil nanocomposite film: Its effect on microbial and sensory quality of lamb meat and growth of common foodborne pathogenic bacteria during refrigeration. *International journal of food microbiology* **251**, 8–14 (2017).
52. Commission, E. Commission Regulation (EU) No 10/2011 of 14 January 2011 on plastic materials and articles intended to come into contact with food. *Off J Eur Union* **12**, 1–89 (2011).
53. Lu, P.-J., Huang, S.-C., Chen, Y.-P., Chiueh, L.-C. & Shih, D. Y.-C. Analysis of titanium dioxide and zinc oxide nanoparticles in cosmetics. *Journal of food and drug analysis* **23**, 587–594 (2015).
54. Zhang, Q., Fan, W. & Gao, L. Anatase TiO2 nanoparticles immobilized on ZnO tetrapods as a highly efficient and easily recyclable photocatalyst. *Applied Catalysis B: Environmental* **76**, 168–173 (2007).
55. Zhou, J., Wang, S. & Gunasekaran, S. Preparation and characterization of whey protein film incorporated with TiO2 nanoparticles. *Journal of food science* **74**, N50–N56 (2009).
56. Khatamiana, M., Divband, B. & Daryana, M. Preparation, characterization and antimicrobial property of ag+-nano Chitosan/ZSM-5: novel Hybrid Biocomposites. *Nanomedicine Journal* **3**, 268–279 (2016).
57. Ojeda-Sana, A. M., van Baren, C. M., Elechosa, M. A., Juárez, M. A. & Moreno, S. New insights into antibacterial and antioxidant activities of rosemary essential oils and their main components. *Food Control* **31**, 189–195 (2013).
58. Zhang, H., Kong, B., Xiong, Y. L. & Sun, X. Antimicrobial activities of spice extracts against pathogenic and spoilage bacteria in modified atmosphere packaged fresh pork and vacuum packaged ham slices stored at 4 C. *Meat science* **81**, 686–692 (2009).
59. Luo, Z., Qin, Y. & Ye, Q. Effect of nano-TiO2-LDPE packaging on microbiological and physicochemical quality of Pacific white shrimp during chilled storage. *International Journal of Food Science & Technology* **50**, 1567–1573 (2015).
60. Han, K. & Yu, M. Study of the preparation and properties of UV-blocking fabrics of a PET/TiO2 nanocomposite prepared by *in situ* polycondensation. *Journal of Applied Polymer Science* **100**, 1588–1593 (2006).
61. Kaneko, M. *et al*. Photoelectrochemical reaction of biomass and bio-related compounds with nanoporous TiO2 film photoanode and O2-reducing cathode. *Electrochemistry Communications* **8**, 336–340 (2006).
62. Yemmireddy, V. K., Farrell, G. D. & Hung, Y. C. Development of titanium dioxide (TiO2) nanocoatings on food contact surfaces and method to evaluate their durability and photocatalytic bactericidal property. *Journal of food science* **80** (2015).
63. Alizadeh-Sani, M., Khezerlou, A. & Ehsani, A. Fabrication and characterization of the bionanocomposite film based on whey protein biopolymer loaded with TiO2 nanoparticles, cellulose nanofibers and rosemary essential oil. *Industrial crops and products* **124**, 300–315 (2018).

64. Haghighi, F., Roudbar Mohammadi, S., Mohammadi, P., Hosseinkhani, S. & Shipour, R. Antifungal activity of TiO2 nanoparticles and EDTA on Candida albicans biofilms. *Infection, Epidemiology and Microbiology* **1**, 33–38 (2013).
65. Bonetta, S., Bonetta, S., Motta, F., Strini, A. & Carraro, E. Photocatalytic bacterial inactivation by TiO2-coated surfaces. *AMB Express* **3**, 59 (2013).
66. Allahverdiyev, A. M., Abamor, E. S., Bagirova, M. & Rafailovich, M. Antimicrobial effects of TiO2 and Ag2O nanoparticles against drug-resistant bacteria and leishmania parasites. *Future microbiology* **6**, 933–940 (2011).
67. Espitia, P. J. P. *et al*. Zinc oxide nanoparticles: synthesis, antimicrobial activity and food packaging applications. *Food and Bioprocess Technology* **5**, 1447–1464 (2012).
68. Sirelkhatim, A. *et al*. Review on zinc oxide nanoparticles: antibacterial activity and toxicity mechanism. *Nano-Micro Letters* **7**, 219–242 (2015).
69. Jones, N., Ray, B., Ranjit, K. T. & Manna, A. C. Antibacterial activity of ZnO nanoparticle suspensions on a broad spectrum of microorganisms. *FEMS microbiology letters* **279**, 71–76 (2008).
70. Franklin, N. M. *et al*. Comparative toxicity of nanoparticulate ZnO, bulk ZnO, and ZnCl2 to a freshwater microalga (Pseudokirchneriella subcapitata): the importance of particle solubility. *Environmental science & technology* **41**, 8484–8490 (2007).
71. Liu, Y. *et al*. Antibacterial activities of zinc oxide nanoparticles against Escherichia coli O157: H7. *Journal of applied microbiology* **107**, 1193–1201 (2009).
72. Besinis, A., De Peralta, T. & Handy, R. D. The antibacterial effects of silver, titanium dioxide and silica dioxide nanoparticles compared to the dental disinfectant chlorhexidine on Streptococcus mutans using a suite of bioassays. *Nanotoxicology* **8**, 1–16 (2014).
73. De Jong, W. H. & Borm, P. J. Drug delivery and nanoparticles: applications and hazards. *International journal of nanomedicine* **3**, 133 (2008).
74. Hernández-Sierra, J. F. *et al*. The antimicrobial sensitivity of Streptococcus mutans to nanoparticles of silver, zinc oxide, and gold. *Nanomedicine: Nanotechnology, Biology and Medicine* **4**, 237–240 (2008).
75. Ruparelia, J. P., Chatterjee, A. K., Duttagupta, S. P. & Mukherji, S. Strain specificity in antimicrobial activity of silver and copper nanoparticles. *Acta biomaterialia* **4**, 707–716 (2008).
76. Slavin, Y. N., Asnis, J. Häfeli, U. O. & Bach, H. Metal nanoparticles: understanding the mechanisms behind antibacterial activity. *Journal of Nanobiotechnology* **15**, https://doi.org/10.1186/s12951-017-0308-z (2017).
77. Rivera-Garza, M., Olguın, M., Garcıa-Sosa, I., Alcántara, D. & Rodrıguez-Fuentes, G. Silver supported on natural Mexican zeolite as an antibacterial material. *Microporous and Mesoporous Materials* **39**, 431–444 (2000).
78. Kawahara, K., Tsuruda, K., Morishita, M. & Uchida, M. Antibacterial effect of silver-zeolite on oral bacteria under anaerobic conditions. *Dental materials* **16**, 452–455 (2000).
79. Administration, F. D. C. ode of Federal Regulations Title 21: Food and drugs chapter I—Food and drug administration department of health and human services subchapter a—general—Part 11: Electronic records; Electronic signatures [Internet]. [cited 2012 Oct 12]. In. (1997).
80. Hashemabad, Z. N., Shabanpour, B., Azizi, H., Ojagh, S. M. & Alishahi, A. Effect of Tio (2) Nanoparticles on the Antibacterial and Physical Properties of Low-Density Polyethylene Film. *Polymer-Plastics Technology and Engineering* **56**, 1516–1527 (2017).
81. Administration, F. D. C. o. o. F. R. T. F. a. d. c. I. Food and drug administration department of health and human services subchapter a-general-Part 11: Electronic records; Electronic signatures [Internet]. [cited 2012 Oct 12]. In. (1997).
82. Lian, Z., Zhang, Y. & Zhao, Y. Nano-TiO2 particles and high hydrostatic pressure treatment for improving functionality of polyvinyl alcohol and chitosan composite films and nano-TiO2 migration from film matrix in food simulants. *Innovative food science & emerging technologies* **33**, 145–153 (2016).

Acknowledgements

The authors would like to thank the Tabriz University of Medical Sciences (TBZMED) (Project No. 61144) for their financial support of this research.

Author contributions

Maryam Azizi-Lalabadi: writing of manuscript. Ali Ehsani: Design of experiment and method. Baharak Divband: Design of experiment and method. Mahmood Alizadeh-Sani: conducted statistical analysis.

Competing interests

The authors declare no competing interests.

Additional information

Supplementary information is available for this paper at https://doi.org/10.1038/s41598-019-54025-0.

Correspondence and requests for materials should be addressed to A.E.

Reprints and permissions information is available at www.nature.com/reprints.

Publisher's note Springer Nature remains neutral with regard to jurisdictional claims in published maps and institutional affiliations.